This is the accepted manuscript made available via CHORUS. The article has been published as:

Measurements of dielectron production in math xmlns="http://www.w3.org/1998/Math/MathML">mrow>mi>Au/mi>mo>+/mo>mi>Au/mi>/mrow>/math> collisions at math xmlns="http://www.w3.org/1998/Math/MathML">mrow>msqrt>msub>mi>s/mi>mrow>mi>N/mi>mi>N/mi>/mrow>/msub>/msqrt>mo>=/mo>mn>27/mn>/mrow>/math>, 39, and 62.4 GeV from the STAR experiment

M. I. Abdulhamid et al. (STAR Collaboration)

Phys. Rev. C **107**, L061901 — Published 1 June 2023

DOI: 10.1103/PhysRevC.107.L061901

Measurements of Dielectron Production in Au+Au Collisions at $\sqrt{s_{NN}}$= 27, 39, and 62.4 GeV from the STAR Experiment

M. I. Abdulhamid,[4] B. E. Aboona,[55] J. Adam,[15] L. Adamczyk,[2] J. R. Adams,[39] I. Aggarwal,[41] M. M. Aggarwal,[41] Z. Ahammed,[62] D. M. Anderson,[55] E. C. Aschenauer,[6] S. Aslam,[26] J. Atchison,[1] V. Bairathi,[53] W. Baker,[11] J. G. Ball Cap,[22] K. Barish,[11] R. Bellwied,[22] P. Bhagat,[29] A. Bhasin,[29] S. Bhatta,[52] J. Bielcik,[15] J. Bielcikova,[38] J. D. Brandenburg,[39] J. Butterworth,[43] X. Z. Cai,[50] H. Caines,[65] M. Calderón de la Barca Sánchez,[9] D. Cebra,[9] J. Ceska,[15] I. Chakaberia,[32] P. Chaloupka,[15] B. K. Chan,[10] Z. Chang,[27] A. Chatterjee,[17] D. Chen,[11] J. Chen,[49] J. H. Chen,[20] Z. Chen,[49] J. Cheng,[57] Y. Cheng,[10] S. Choudhury,[20] W. Christie,[6] X. Chu,[6] H. J. Crawford,[8] M. Csanád,[18] G. Dale-Gau,[13] A. Das,[15] M. Daugherity,[1] I. M. Deppner,[21] A. Dhamija,[41] L. Di Carlo,[64] L. Didenko,[6] P. Dixit,[24] X. Dong,[32] J. L. Drachenberg,[1] E. Duckworth,[30] J. C. Dunlop,[6] J. Engelage,[8] G. Eppley,[43] S. Esumi,[58] O. Evdokimov,[13] A. Ewigleben,[33] O. Eyser,[6] R. Fatemi,[31] S. Fazio,[7] C. J. Feng,[37] Y. Feng,[42] E. Finch,[51] Y. Fisyak,[6] F. A. Flor,[65] C. Fu,[12] C. A. Gagliardi,[55] T. Galatyuk,[16] F. Geurts,[43] N. Ghimire,[54] A. Gibson,[61] K. Gopal,[25] X. Gou,[49] D. Grosnick,[61] Y. Guo,[30] A. Gupta,[29] W. Guryn,[6] A. Hamed,[4] Y. Han,[43] S. Harabasz,[16] M. D. Harasty,[9] J. W. Harris,[65] H. Harrison-Smith,[31] W. He,[20] X. H. He,[28] Y. He,[49] N. Herrmann,[21] L. Holub,[15] C. Hu,[28] Q. Hu,[28] Y. Hu,[32] B. Huang,[13] H. Huang,[37] H. Z. Huang,[10] S. L. Huang,[52] T. Huang,[13] X. Huang,[57] Y. Huang,[57] Y. Huang,[12] P. Huck,[32] T. J. Humanic,[39] D. Isenhower,[1] M. Isshiki,[58] W. W. Jacobs,[27] A. Jalotra,[29] C. Jena,[25] A. Jentsch,[6] Y. Ji,[32] J. Jia,[6,52] C. Jin,[43] X. Ju,[46] E. G. Judd,[8] S. Kabana,[53] M. L. Kabir,[11] S. Kagamaster,[33] D. Kalinkin,[31] K. Kang,[57] D. Kapukchyan,[11] K. Kauder,[6] H. W. Ke,[6] D. Keane,[30] M. Kelsey,[64] Y. V. Khyzhniak,[39] D. P. Kikoła,[63] B. Kimelman,[9] D. Kincses,[18] I. Kisel,[19] A. Kiselev,[6] A. G. Knospe,[33] H. S. Ko,[32] L. K. Kosarzewski,[15] L. Kramarik,[15] L. Kumar,[41] S. Kumar,[28] R. Kunnawalkam Elayavalli,[65] R. Lacey,[52] J. M. Landgraf,[6] J. Lauret,[6] A. Lebedev,[6] J. H. Lee,[6] Y. H. Leung,[21] N. Lewis,[6] C. Li,[49] W. Li,[43] X. Li,[46] Y. Li,[46] Y. Li,[57] Z. Li,[46] X. Liang,[11] Y. Liang,[30] R. Licenik,[38,15] T. Lin,[49] M. A. Lisa,[39] C. Liu,[28] F. Liu,[12] G. Liu,[47] H. Liu,[27] H. Liu,[12] L. Liu,[12] T. Liu,[65] X. Liu,[39] Y. Liu,[55] Z. Liu,[12] T. Ljubicic,[6] W. J. Llope,[64] O. Lomicky,[15] R. S. Longacre,[6] E. M. Loyd,[11] T. Lu,[28] N. S. Lukow,[54] X. F. Luo,[12] L. Ma,[20] R. Ma,[6] Y. G. Ma,[20] N. Magdy,[52] D. Mallick,[36] S. Margetis,[30] C. Markert,[56] H. S. Matis,[32] J. A. Mazer,[44] G. McNamara,[64] K. Mi,[12] S. Mioduszewski,[55] B. Mohanty,[36] M. M. Mondal,[36] I. Mooney,[65] A. Mukherjee,[18] M. I. Nagy,[18] A. S. Nain,[41] J. D. Nam,[54] Md. Nasim,[24] D. Neff,[10] J. M. Nelson,[8] D. B. Nemes,[65] M. Nie,[49] T. Niida,[58] R. Nishitani,[58] T. Nonaka,[58] G. Odyniec,[32] A. Ogawa,[6] S. Oh,[48] K. Okubo,[58] B. S. Page,[6] R. Pak,[6] J. Pan,[55] A. Pandav,[36] A. K. Pandey,[28] T. Pani,[44] A. Paul,[11] B. Pawlik,[40] D. Pawlowska,[63] C. Perkins,[8] J. Pluta,[63] B. R. Pokhrel,[54] M. Posik,[54] T. Protzman,[33] V. Prozorova,[15] N. K. Pruthi,[41] M. Przybycien,[2] J. Putschke,[64] Z. Qin,[57] H. Qiu,[28] A. Quintero,[54] C. Racz,[11] S. K. Radhakrishnan,[30] N. Raha,[64] R. L. Ray,[56] R. Reed,[33] H. G. Ritter,[32] C. W. Robertson,[42] M. Robotkova,[38,15] M. A. Rosales Aguilar,[31] D. Roy,[44] P. Roy Chowdhury,[63] L. Ruan,[6] A. K. Sahoo,[24] N. R. Sahoo,[49] H. Sako,[58] S. Salur,[44] S. Sato,[58] W. B. Schmidke,[6] N. Schmitz,[34] F-J. Seck,[16] J. Seger,[14] R. Seto,[11] P. Seyboth,[34] N. Shah,[26] P. V. Shanmuganathan,[6] T. Shao,[20] M. Sharma,[29] N. Sharma,[24] R. Sharma,[25] S. R. Sharma,[25] A. I. Sheikh,[30] D. Y. Shen,[20] K. Shen,[46] S. S. Shi,[12] Y. Shi,[49] Q. Y. Shou,[20] F. Si,[46] J. Singh,[41] S. Singha,[28] P. Sinha,[25] M. J. Skoby,[5,42] N. Smirnov,[65] Y. Söhngen,[21] Y. Song,[65] B. Srivastava,[42] T. D. S. Stanislaus,[61] M. Stefaniak,[39] D. J. Stewart,[64] B. Stringfellow,[42] Y. Su,[46] A. A. P. Suaide,[45] M. Sumbera,[38] C. Sun,[52] X. Sun,[28] Y. Sun,[46] Y. Sun,[23] B. Surrow,[54] Z. W. Sweger,[9] P. Szymanski,[63] A. Tamis,[65] A. H. Tang,[6] Z. Tang,[46] T. Tarnowsky,[35] J. H. Thomas,[32] A. R. Timmins,[22] D. Tlusty,[14] T. Todoroki,[58] C. A. Tomkiel,[33] S. Trentalange,[10] R. E. Tribble,[55] P. Tribedy,[6] T. Truhlar,[15] B. A. Trzeciak,[15] O. D. Tsai,[10,6] C. Y. Tsang,[30,6] Z. Tu,[6] T. Ullrich,[6] D. G. Underwood,[3,61] I. Upsal,[43] G. Van Buren,[6] J. Vanek,[6] I. Vassiliev,[19] V. Verkest,[64] F. Videbæk,[6] S. A. Voloshin,[64] F. Wang,[42] G. Wang,[10] J. S. Wang,[23] X. Wang,[49] Y. Wang,[46] Y. Wang,[12] Y. Wang,[57] Z. Wang,[49] J. C. Webb,[6] P. C. Weidenkaff,[21] G. D. Westfall,[35] D. Wielanek,[63] H. Wieman,[32] G. Wilks,[13] S. W. Wissink,[27] R. Witt,[60] J. Wu,[12] J. Wu,[28] X. Wu,[10] Y. Wu,[11] B. Xi,[50] Z. G. Xiao,[57] G. Xie,[59] W. Xie,[42] H. Xu,[23] N. Xu,[32] Q. H. Xu,[49] Y. Xu,[49] Y. Xu,[12] Z. Xu,[6] Z. Xu,[10] G. Yan,[49] Z. Yan,[52] C. Yang,[49] Q. Yang,[49] S. Yang,[47] Y. Yang,[37] Z. Ye,[43] Z. Ye,[13] L. Yi,[49] K. Yip,[6] Y. Yu,[49] H. Zbroszczyk,[63] W. Zha,[46] C. Zhang,[52] D. Zhang,[12] J. Zhang,[49] S. Zhang,[46] W. Zhang,[47] X. Zhang,[28] Y. Zhang,[28] Y. Zhang,[46] Y. Zhang,[12] Z. J. Zhang,[37] Z. Zhang,[6] Z. Zhang,[13] F. Zhao,[28] J. Zhao,[20] M. Zhao,[6] C. Zhou,[20] J. Zhou,[46] S. Zhou,[12] Y. Zhou,[12] X. Zhu,[57] M. Zurek,[3,6] and M. Zyzak[19]

(STAR Collaboration)

[1] *Abilene Christian University, Abilene, Texas 79699*
[2] *AGH University of Science and Technology, FPACS, Cracow 30-059, Poland*
[3] *Argonne National Laboratory, Argonne, Illinois 60439*

[4] *American University of Cairo, New Cairo 11835, New Cairo, Egypt*
[5] *Ball State University, Muncie, Indiana, 47306*
[6] *Brookhaven National Laboratory, Upton, New York 11973*
[7] *University of Calabria & INFN-Cosenza, Rende 87036, Italy*
[8] *University of California, Berkeley, California 94720*
[9] *University of California, Davis, California 95616*
[10] *University of California, Los Angeles, California 90095*
[11] *University of California, Riverside, California 92521*
[12] *Central China Normal University, Wuhan, Hubei 430079*
[13] *University of Illinois at Chicago, Chicago, Illinois 60607*
[14] *Creighton University, Omaha, Nebraska 68178*
[15] *Czech Technical University in Prague, FNSPE, Prague 115 19, Czech Republic*
[16] *Technische Universität Darmstadt, Darmstadt 64289, Germany*
[17] *National Institute of Technology Durgapur, Durgapur - 713209, India*
[18] *ELTE Eötvös Loránd University, Budapest, Hungary H-1117*
[19] *Frankfurt Institute for Advanced Studies FIAS, Frankfurt 60438, Germany*
[20] *Fudan University, Shanghai, 200433*
[21] *University of Heidelberg, Heidelberg 69120, Germany*
[22] *University of Houston, Houston, Texas 77204*
[23] *Huzhou University, Huzhou, Zhejiang 313000*
[24] *Indian Institute of Science Education and Research (IISER), Berhampur 760010 , India*
[25] *Indian Institute of Science Education and Research (IISER) Tirupati, Tirupati 517507, India*
[26] *Indian Institute Technology, Patna, Bihar 801106, India*
[27] *Indiana University, Bloomington, Indiana 47408*
[28] *Institute of Modern Physics, Chinese Academy of Sciences, Lanzhou, Gansu 730000*
[29] *University of Jammu, Jammu 180001, India*
[30] *Kent State University, Kent, Ohio 44242*
[31] *University of Kentucky, Lexington, Kentucky 40506-0055*
[32] *Lawrence Berkeley National Laboratory, Berkeley, California 94720*
[33] *Lehigh University, Bethlehem, Pennsylvania 18015*
[34] *Max-Planck-Institut für Physik, Munich 80805, Germany*
[35] *Michigan State University, East Lansing, Michigan 48824*
[36] *National Institute of Science Education and Research, HBNI, Jatni 752050, India*
[37] *National Cheng Kung University, Tainan 70101*
[38] *Nuclear Physics Institute of the CAS, Rez 250 68, Czech Republic*
[39] *The Ohio State University, Columbus, Ohio 43210*
[40] *Institute of Nuclear Physics PAN, Cracow 31-342, Poland*
[41] *Panjab University, Chandigarh 160014, India*
[42] *Purdue University, West Lafayette, Indiana 47907*
[43] *Rice University, Houston, Texas 77251*
[44] *Rutgers University, Piscataway, New Jersey 08854*
[45] *Universidade de São Paulo, São Paulo, Brazil 05314-970*
[46] *University of Science and Technology of China, Hefei, Anhui 230026*
[47] *South China Normal University, Guangzhou, Guangdong 510631*
[48] *Sejong University, Seoul, 05006, South Korea*
[49] *Shandong University, Qingdao, Shandong 266237*
[50] *Shanghai Institute of Applied Physics, Chinese Academy of Sciences, Shanghai 201800*
[51] *Southern Connecticut State University, New Haven, Connecticut 06515*
[52] *State University of New York, Stony Brook, New York 11794*
[53] *Instituto de Alta Investigación, Universidad de Tarapacá, Arica 1000000, Chile*
[54] *Temple University, Philadelphia, Pennsylvania 19122*
[55] *Texas A&M University, College Station, Texas 77843*
[56] *University of Texas, Austin, Texas 78712*
[57] *Tsinghua University, Beijing 100084*
[58] *University of Tsukuba, Tsukuba, Ibaraki 305-8571, Japan*
[59] *University of Chinese Academy of Sciences, Beijing, 101408*
[60] *United States Naval Academy, Annapolis, Maryland 21402*
[61] *Valparaiso University, Valparaiso, Indiana 46383*
[62] *Variable Energy Cyclotron Centre, Kolkata 700064, India*
[63] *Warsaw University of Technology, Warsaw 00-661, Poland*
[64] *Wayne State University, Detroit, Michigan 48201*
[65] *Yale University, New Haven, Connecticut 06520*

We report systematic measurements of dielectron (e^+e^-) invariant-mass M_{ee} spectra at mid-rapidity in Au+Au collisions at $\sqrt{s_{NN}}$ = 27, 39, and 62.4 GeV taken with the STAR detector at the Relativistic Heavy Ion Collider. For all energies studied, a significant excess yield of dielectrons is observed in the low-mass region ($0.40< M_{ee} < 0.75$ MeV/c^2) compared to hadronic cocktail simulations at freeze-out. Models that include an in-medium broadening of the ρ-meson spectral function consistently describe the observed excess. In addition, we report acceptance-corrected dielectron-excess spectra for Au+Au collisions at mid-rapidity ($|y_{ee}| < 1$) in the 0−80% centrality bin for each collision energy. The integrated excess yields for $0.4 < M_{ee} < 0.75$ GeV/c^2, normalized by the charged particle multiplicity at mid-rapidity, are compared with previously published measurements for Au+Au at $\sqrt{s_{NN}}$ = 19.6 and 200 GeV. Models that include an in-medium broadening of the ρ-meson spectral function consistently describe the observed excess. The normalized excess yields in the low-mass region show no significant collision energy dependence. The data, however, are consistent with model calculations that demonstrate a modest energy dependence.

Experimentally, dileptons are good probes of the hot quantum chromodynamics (QCD) medium created in heavy-ion collisions because leptons are not affected by the strong interaction. As a result, leptons can traverse the hot medium with minimal final-state effects, providing means to experimentally test models that predict chiral symmetry restoration and enable a better understanding of the microscopic properties of QCD matter.

The generation of hadronic masses is in part caused by the spontaneous breaking of chiral symmetry [1, 2]. Ultrarelativistic heavy-ion collisions produce a hot and dense QCD medium, a Quark-Gluon Plasma (QGP), where partial chiral symmetry restoration is expected [3]. Theoretical calculations suggest that chiral symmetry restoration will result in the modification of chiral partners such as the $\rho(770)$ vector meson and the $a_1(1260)$ axial-vector meson [4] with subsequent ρ and a_1 mass degeneracy. Reconstruction of the a_1 is an experimentally challenging task with its broad resonance width and decay daughter(s) (e.g., π) that rescatter in the QCD medium. The ρ, however, can be reconstructed through its leptonic e^+e^- decay channel, allowing its spectral distribution to be studied.

The CERES Collaboration at the Super Proton Synchrotron observed an excess yield in Pb+Au collisions at $\sqrt{s_{NN}}$ = 8 and 17.3 GeV [5, 6] in the low dielectron (unlike-sign pairs unless otherwise specified) invariant mass range (LMR) (i.e., below the ϕ meson mass), where excess yield is the difference between the measured yield and an expected yield based on simulations. The excess yield in the LMR was observed relative to known hadronic sources, including the $\rho-$decay in vacuum. High-precision dimuon measurements in In+In collisions by the NA60 Collaboration at $\sqrt{s_{NN}}$ = 17.3 GeV suggest that the observed LMR excess is consistent with the in-medium broadening of the ρ spectral function [7]. At the Relativistic Heavy Ion Collider (RHIC), measurements of dielectron mass spectra in Au+Au collisions at $\sqrt{s_{NN}}$ = 200 GeV show a significant excess in the LMR when compared to the known hadronic sources. The excess has been observed by both the STAR and PHENIX Collaborations [8–12]. Theoretical calculations using a many-body approach [13] or a transport model [14, 15] predict an in-medium broadened ρ spectral function, and both calculations are consistent with the previously published STAR and ALICE results from Au+Au at $\sqrt{s_{NN}}$ = 200 GeV and Pb+Pb at $\sqrt{s_{NN}}$ = 5.02 TeV [16], respectively.

The RHIC Beam Energy Scan (BES) program [17] provides a unique opportunity to systematically test these calculations as a function of the initial collision energy. In the BES energy range between $\sqrt{s_{NN}}$ = 27 and 62.4 GeV we observe the freeze-out temperature [1] to remain constant [18]. Moreover, we find the total baryon density to remain approximately constant, based on the yield ratio of protons and anti-protons to charged pions [18, 19]. Both will serve here as a baseline to test the aforementioned theoretical calculations against.

In this Letter, the STAR Collaboration presents the first measurements of dielectron production in Au+Au collisions with colliding nucleon + nucleon pair energy ($\sqrt{s_{NN}}$) at 27, 39, and 62.4 GeV. The data were collected by the STAR detector in the 2010 and 2011 RHIC runs using a minimum-bias trigger which requires a coincidence of signals in the -z and +z components of either the vertex position detector, beam-beam counters, or the zero degree calorimeters. The analyses included 68M, 132M, and 62M collision events for $\sqrt{s_{NN}}$ = 27 GeV, 39 GeV, and 62.4 GeV, respectively. The main detector systems involved in this analysis are the Time Projection Chamber (TPC) [20] and the Time-Of-Flight (TOF) detectors [21]. We report the LMR acceptance-corrected excess yields for the 80% most-central collisions.

Electron identification was performed using methods described in [9]. The TPC is used for electron identification via energy-loss measurements, and in conjunction with the TOF, the electron signal is improved by removing slow hadrons. The purity of the electron samples is 95% for 62.4 GeV and 94% for the other two energies. The invariant mass spectrum for dielectrons was generated using all accepted, oppositely-charged electron candidate pairs from the same event and summing over all events. Only electrons with pseudo-rapidity $|\eta^e| < 1$ and transverse momentum $p_T^e > 0.2$ GeV/c were used in this analysis. The dielectrons from photon conversion

[1] The temperature of the expanding QCD matter when nuclear scatterings cease.

in the detector materials were greatly suppressed by requiring a minimum pair opening angle, as described in [9, 11]. The like-sign combination method was adopted to reproduce the background because it simultaneously reproduces correlated and uncorrelated sources [11]. The background subtraction was performed as a function of M_{ee} and pair momentum p_T^{ee}.

The raw data were corrected for the single-electron reconstruction efficiency as well as for the loss of dielectrons in the very low-mass region $M_{ee} < 0.2$ GeV/c^2 caused by the minimum opening angle requirement. An embedding technique was used to determine the tracking efficiency [9, 10], while the electron identification efficiency was derived from data- driven techniques [9]. The single-electron reconstruction efficiency was folded into the pair efficiency via a virtual photon method [10] and applied to the background- subtracted dielectron spectrum in M_{ee} and p_T^{ee}.

The systematic uncertainties in the final mass spectra include uncertainties in (*i*) the acceptances for like-sign and unlike-sign dielectrons, (*ii*) the hadron contamination, and (*iii*) the efficiency corrections [9]. The dominant systematic uncertainty contribution in the LMR, the efficiency correction uncertainty is 8%, 7.7%, and 10.8% for $\sqrt{s_{NN}}$ = 27, 39, and 62.4 GeV, respectively. For masses greater than the ϕ mass, the hadron contamination uncertainty is of the same order as the efficiency-corrections uncertainty. The uncertainty in the acceptance factor begins to contribute significantly above $\sim$2 GeV/c^2. The sources of uncertainty are added together in quadrature to determine the total systematic uncertainty as a function of M_{ee}.

The hadronic sources for dielectrons were simulated using the method described in [9, 10], where the meson yields follow the method in [10]. They include contributions from direct and/or Dalitz decays of π^0, η, η', ω, ϕ, J/ψ mesons, as well as contributions from $c\bar{c}$ and Drell-Yan (DY) decays. The input p_T spectral shapes were created using Tsallis Blast-Wave (TBW) parameterizations [22] based on STAR measurements of light hadron production. The J/ψ p_T spectra were estimated for $\sqrt{s_{NN}}$ = 39 and 62.4 GeV using Boltzmann parameterizations which were based on published data [23], while the $\sqrt{s_{NN}}$ = 27 GeV spectra were estimated using the same parameterization as for the $\sqrt{s_{NN}}$ = 39 GeV data.

The semi-leptonic decays of charmed hadrons in p+p collisions were simulated using PYTHIA v6.416 [24] with the tune described in [25]. The perturbative QCD fixed-order plus next-to-leading logarithms upper-limit [6, 26] was used to fit the world-wide measurements of $\sigma_{c\bar{c}}^{NN}$ [27] in order to determine the input charm production cross-section. The $\sigma_{c\bar{c}}^{NN}$ values estimated from the fit are 17 $\pm$ 6 μb, 37 $\pm$ 2 μb, and 91 $\pm$ 6 μb for $\sqrt{s_{NN}}$ = 27, 39, and 62.4 GeV, respectively. The obtained charm-related distribution was scaled by the number of nucleon-nucleon binary collisions $N_{\rm bin}$ [28] to obtain an estimate of the charm contribution in minimum-bias (0$-$80% centrality) Au+Au collisions [10]. The DY contribution was estimated following the procedure used in [9]. However, $\sigma_{DY}^{pp}(\sqrt{s})$ was taken from PYTHIA and was corrected by the ratio of the cross section used in [10] to the corresponding PYTHIA cross-section at $\sqrt{s}$ = 19.6 GeV.

The efficiency-corrected spectra are shown in Fig. 1 for 0$-$80% most-central Au+Au collisions at $\sqrt{s_{NN}}$ = 27, 39, and 62.4 GeV. The figure shows p_T-integrated invariant mass spectra captured in the STAR acceptance at mid-rapidity ($|\eta^e| < 1$, $p_T^e > 0.2$ GeV/c, and $|y_{ee}| < 1$), where each data point is positioned at the bin center and the bin markers parallel to the x-axis indicate the bin width. The data are compared to a hadronic cocktail without the vacuum ρ-meson since its contributions are expected to be strongly modified in the medium. To illustrate the extent of STAR's systematic study of e^+e^- production, Fig. 1 includes the efficiency-corrected spectra for the 0$-$80% most-central Au+Au collisions at $\sqrt{s_{NN}}$ = 19.6 and 200 GeV from Refs. [9, 10].

Figure 2 shows the ratio of the present data to the hadronic cocktail with the yields from ω and ϕ subtracted from both the data and cocktail. The open boxes depict the experimental systematic uncertainties, while the gray bands represent the cocktail simulation uncertainties. To keep the data and cocktail uncertainties separate throughout this study, the ω and ϕ yield uncertainties remain in the cocktail uncertainties. A clear enhancement is observed in the LMR relative to the hadronic cocktail for each of the three collision energies.

Model calculations within the STAR acceptance by Rapp *et al.* [13, 29], Endres *et al.* [30], and calculations using the PHSD model [14, 15] were separately added to the hadronic cocktail and the resulting combined spectra are compared to the reference cocktail, via ratios, as shown in Fig. 2. The model by Rapp *et al.* is an effective many-body calculation for vector mesons where the spectral function of ρ is modified (broadened) primarily due to interactions with baryons and mesons (i.e., a hadron gas). The model by Endres *et al.* is a coarse-grained transport approach that includes the ρ spectral function mentioned above from [13, 31]. PHSD is a microscopic transport model which includes the collisional broadening of the ρ. Each model has successfully described the LMR $\mu^+\mu^-$ excess yield observed by the NA60 experiment, as well as measurements of Au+Au collisions at $\sqrt{s_{NN}}$ = 200 GeV [8, 12, 13, 15, 30]. Each model includes thermal contributions from the in-medium broadening of the ρ spectral function and a QGP. In contrast to the models in [13, 29, 30], the PHSD model includes an incoherent sum of contributions from the ρ, the QGP, and Dalitz decays of the a_1 and Δ resonances. These contributions tend to underestimate the e^+e^- yield for $M_{ee} < 0.3$ GeV/c^2. However, we note that these PHSD model calculations do not include Bremsstrahlung processes [15].

To further quantify the excess in the LMR, cocktail contributions excluding the ρ-meson were subtracted from the dielectron yields. The excess spectra were corrected for the STAR acceptance using a virtual photon

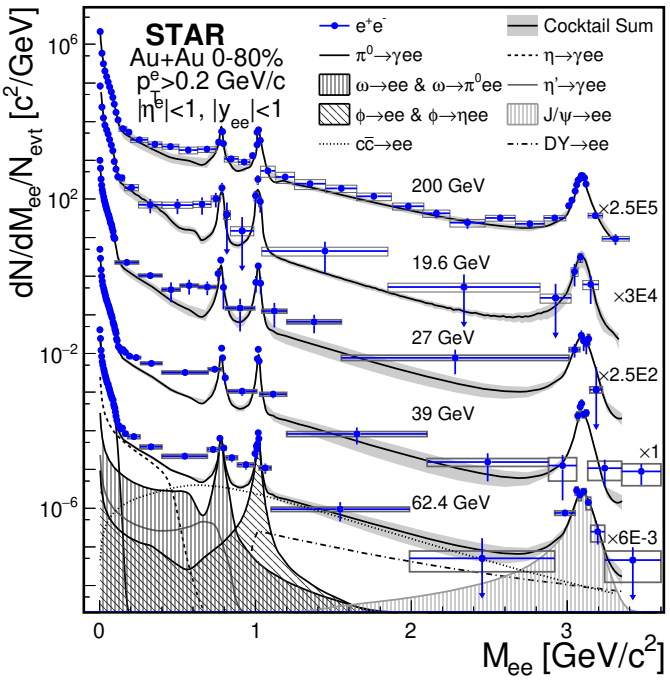


FIG. 1. Background subtracted dielectron invariant mass spectra within the STAR acceptance from $\sqrt{s_{NN}}$ = 19.6, 27, 39, 62.4, and 200 GeV 0−80% most-central Au+Au collisions. Errors bars and open boxes represent the statistical and systematic uncertainties in the measurements. The solid black curves represent the hadronic cocktail, with the gray bands representing the cocktail uncertainties. The curves underneath the $\sqrt{s_{NN}}$ = 62.4 GeV hadronic cocktail curve and gray band represent the cocktail components at 62.4 GeV. For better presentation, the measurements and cocktail predictions are not listed in order by energy but have been scaled by factors 2.5×10^5, 3×10^4, 2.5×10^2, 1, and 6×10^{-3} for results at $\sqrt{s_{NN}}$ = 200, 19.6, 27, 39, and 62.4 GeV, respectively.

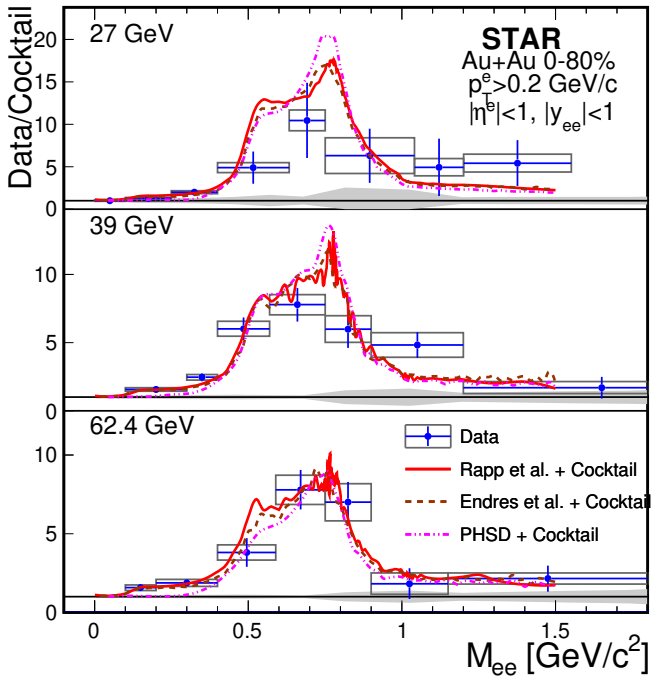


FIG. 2. The ratio of the invariant mass spectra to the cocktail with the ω and ϕ yields removed from both the data and cocktail. The gray area shows the cocktail uncertainties. Model calculations by Rapp *et al.* [13], Endres *et al.* [30], and PHSD [14, 15] were separately added to the reference cocktail and compared to the reference cocktail, via ratios, as shown with the curves.

method similar to that described in [10]. The corrected excess yields were then normalized to the charged particle multiplicities at mid-rapidity[2] (dN_{ch}/dy) in order to cancel out the volume effect. Figure 3 shows the acceptance-corrected excess spectra. Systematic uncertainties from the measurements and the cocktail are shown in the figure as the open and filled boxes, respectively. The 6% uncertainty from STAR's acceptance correction and the uncertainty of dN_{ch}/dy are not shown in the figure. Model calculations [13–15] in Fig. 3 include contributions from broadening of the ρ spectral function in a hadron gas (Rapp Rho) and from QGP radiation (Rapp QGP). The PHSD model calculations in Fig. 3 include contributions from the ρ meson (PHSD Rho), QGP (PHSD QGP), Dalitz decays of the a_1 (PHSD a1), and Δ resonances (PHSD Delta). The sums (Rapp Sum, PHSD Sum) are compared with the excess yield at each energy. Calculations by Rapp *et al.* have an uncertainty on the order of 15% [13], and PHSD model calculations have an uncertainty on the order of 30% [32]. Within uncertainties, the model calculations are found to reproduce the acceptance-corrected excess in Au+Au collisions at each of the collision energies.

To allow for a direct comparison of our measurements with previously published results and model calculations, we integrated the acceptance-corrected dielectron excess spectra in the mass region from 0.40 to 0.75 GeV/c^2. Figure 4 shows the integrated excess yields normalized by dN_{ch}/dy from the 0−80% most-central Au+Au collisions at $\sqrt{s_{NN}}$ = 27, 39, and 62.4 GeV, together with our previously published results [10] for the 0−80% most-central Au+Au collisions at $\sqrt{s_{NN}}$ = 19.6 and 200 GeV. In addition, we compare to the NA60 $\mu^+\mu^-$ measurement at $\sqrt{s_{NN}}$ = 17.3 GeV for $dN_{ch}/d\eta > 30$ [33][3]. For the measurements at $\sqrt{s_{NN}}$ = 27, 39, and 62.4 GeV, the systematic uncertainties from the data and cocktail are shown as the open and filled boxes, respectively.

[2] For Au+Au collisions at $\sqrt{s_{NN}}$ = 27 and 39 GeV, dN_{ch}/dy is approximated by the dN/dy sum of $\pi^\pm$, $K^\pm$, p, and $\bar{p}$ [18]. For $\sqrt{s_{NN}}$= 62.4 GeV, dN_{ch}/dy is given in [19].

[3] NA60 measurements in [7] have been updated in [33]. This paper uses the updated measurements while [10] used the previous measurements. Additionally, dN_{ch}/dy = 120 is used, where dN_{ch}/dy = 140 was used in [10].

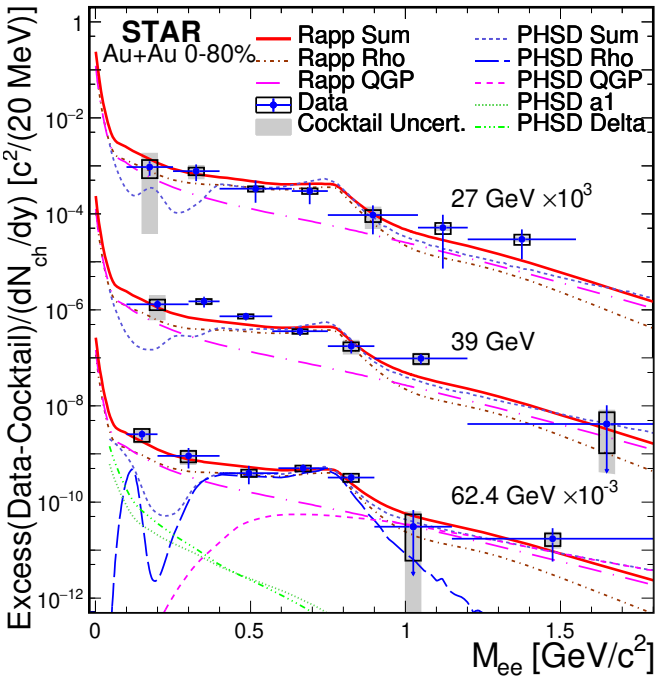


FIG. 3. Acceptance-corrected dielectron excess mass spectra, normalized by dN_{ch}/dy, for Au+Au collisions at $\sqrt{s_{NN}}$ = 27, 39, and 62.4 GeV. Model calculations (curves) [13–15] are compared with the excess spectra for each energy, as explained in the text. Individual components of the PHSD model calculations are only shown for Au+Au collisions at $\sqrt{s_{NN}}$ = 62.4 GeV. The error bars, open boxes, and filled boxes indicate statistical, systematic, and cocktail uncertainties. A 6% uncertainty on the acceptance correction is not shown.

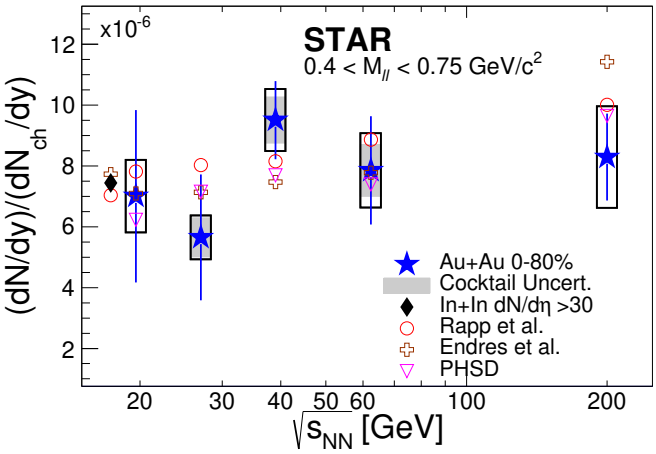


FIG. 4. Collision energy dependence of the integrated dilepton excess yields in 0.4 < M_{ll} < 0.75 GeV/c^2, normalized by dN_{ch}/dy. The closed markers represent the experimental measurements, while the open markers represent the calculations from Rapp *et al.*, Endres *et al.*, and PHSD. For measurements at $\sqrt{s_{NN}}$ = 27, 39, and 62.4 GeV, the open and filled (gray) boxes represent the systematic errors in the measurements and the cocktail uncertainties, respectively. The 6% uncertainty from the acceptance correction is not included. For measurements of minimum-bias, 0−80% central Au+Au collisions at $\sqrt{s_{NN}}$ = 19.6 and 200 GeV, the open boxes represent the total systematic uncertainty in the measurements.

For the measurements at $\sqrt{s_{NN}}$ = 19.6 and 200 GeV, the total (cocktail+data) systematic uncertainties are shown as the open boxes. The normalized, integral yields from model calculations, shown in Fig. 4, agree with the measurements. Note that the result for Au+Au at $\sqrt{s_{NN}}$ = 19.6 GeV [10] is consistent within uncertainties with the $\mu^+\mu^-$ measurement from NA60 in In+In collision at $\sqrt{s_{NN}}$ = 17.3 GeV [7, 33].

The normalized integrated excess yields show no statistically significant collision-energy dependence for the 0-80% most-central Au+Au collisions. This may be because dilepton production in the medium is expected to be mainly determined by the strong coupling of the ρ-meson to baryons, rather than to mesons [4]. We know that the total baryon density remains approximately unchanged for minimum-bias Au+Au collisions with collision energies above $\sqrt{s_{NN}}$ = 20 GeV [18]. However, the models and our data are statistically consistent even though the model predictions display modest energy dependence.

In summary, we have reported dielectron yields for the 0−80% most-central Au+Au collisions at $\sqrt{s_{NN}}$ = 27, 39, and 62.4 GeV. The data were collected with the STAR detector at RHIC. The new measurements complement the previously published results [8–10, 12] and the combined data sets now cover an order-of-magnitude range in collision energies over which the total baryon density and freeze-out temperatures are remarkably constant [18]. Across the collision energies, we have observed statistically significant excesses in the LMR when comparing the data to hadronic cocktails that do not include vacuum ρ decay contributions. The excess yields have been corrected for acceptance, normalized by dN_{ch}/dy, integrated from 0.40 to 0.75 GeV/c^2, and reported as a function of $\sqrt{s_{NN}}$. The measured yields show no significant energy dependence and are statistically consistent with model calculations.

While restricted to the ρ-meson mass range and limited by statistical and systematic uncertainties, our findings are consistent with models that include ρ broadening in the approach to chiral symmetry restoration [34]. Further experimental tests of the models discussed in this paper are warranted.

As part of the Beam Energy Scan Phase II project, the STAR Collaboration has collected over an order of magnitude more data than previously acquired in the energy range from 7.7 to 19.6 GeV, where the total baryon density changes substantially [18]. Future studies may therefore allow us to better understand the competing factors that play a role in the LMR dielectron excess production [29] and to further clarify the connection between ρ-meson broadening and chiral symmetry restoration.

ACKNOWLEDGMENTS

We thank S. Endres, O. Linnyk, E. L. Bratkovskaya, and R. Rapp for discussions and model calculations. We thank the RHIC Operations Group and RCF at BNL, the NERSC Center at LBNL, and the Open Science Grid consortium for providing resources and support. This work was supported in part by the Office of Nuclear Physics within the U.S. DOE Office of Science, the U.S. National Science Foundation, National Natural Science Foundation of China, Chinese Academy of Science, the Ministry of Science and Technology of China and the Chinese Ministry of Education, the Higher Education Sprout Project by Ministry of Education at NCKU, the National Research Foundation of Korea, Czech Science Foundation and Ministry of Education, Youth and Sports of the Czech Republic, Hungarian National Research, Development and Innovation Office, New National Excellency Programme of the Hungarian Ministry of Human Capacities, Department of Atomic Energy and Department of Science and Technology of the Government of India, the National Science Centre and WUT ID-UB of Poland, the Ministry of Science, Education and Sports of the Republic of Croatia, German Bundesministerium für Bildung, Wissenschaft, Forschung and Technologie (BMBF), Helmholtz Association, Ministry of Education, Culture, Sports, Science, and Technology (MEXT) and Japan Society for the Promotion of Science (JSPS).

[1] C. D. Roberts, M. S. Bhagwat, A. Höll, and S. V. Wright, Eur. Phys. J. Spec. Top. **140**, 53 (2007).

[2] S. Aoki et al. (FLAG Collaboration), Eur. Phys. J. C **74**, 2890 (2014).

[3] A. Bazavov, T. Bhattacharya, M. Cheng, C. DeTar, H.-T. Ding, S. Gottlieb, R. Gupta, P. Hegde, U. M. Heller, F. Karsch, et al. (HotQCD Collaboration), Phys. Rev. D **85**, 054503 (2012).

[4] R. Rapp, J. Wambach, and H. van Hees, in *Relativistic Heavy Ion Physics*, edited by R. Stock (Springer-Verlag, 2010), vol. 23 of *Group I: Elementary Particles, Nuclei and Atoms*, chap. 4, pp. 1–42.

[5] D. Adamová et al. (CERES/NA45 Collaboration), Phys. Rev. Lett. **91**, 042301 (2003).

[6] D. Adamova et al. (CERES Collaboration), Phys. Lett. B **666**, 425 (2008).

[7] R. Arnaldi et al. (NA60 Collaboration), Eur. Phys. J. C **61**, 711 (2009).

[8] L. Adamczyk et al. (STAR Collaboration), Phys. Rev. Lett. **113**, 022301 (2014).

[9] L. Adamczyk et al. (STAR Collaboration), Phys. Rev. C **92**, 024912 (2015).

[10] L. Adamczyk et al. (STAR Collaboration), Phys. Lett. B **750**, 64 (2015).

[11] A. Adare et al. (PHENIX Collaboration), Phys. Rev. C **81**, 034911 (2010).

[12] A. Adare et al. (PHENIX Collaboration), Phys. Rev. C **93**, 014904 (2016).

[13] R. Rapp, Phys. Rev. C **63**, 054907 (2001).
H. van Hees and R. Rapp, Phys. Rev. Lett. **97**, 102301 (2006).
H. van Hees and R. Rapp, Nucl. Phys. **A806**, 339 (2008).
R. Rapp, Advances in High Energy Physics **2013**, 148253 (2013).
R. Rapp, private communication (2016).

[14] W. Cassing and E. L. Bratkovskaya, Nucl. Phys. **A831**, 215 (2009).
E. L. Bratkovskaya, W. Cassing, V. P. Konchakovski, and O. Linnyk, Nucl. Phys. **A856**, 162 (2011).
O. Linnyk, W. Cassing, J. Manninen, E. L. Bratkovskaya, and C. M. Ko, Phys. Rev. C **85**, 024910 (2012).

[15] O. Linnyk, E. L. Bratkovskaya, and W. Cassing, Prog. Part. Nucl. Phys. **87**, 50 (2016).

[16] S. Acharya et al. (ALICE), Phys. Rev. C **99**, 024002 (2019), 1807.00923.

[17] STAR Note **SN0493** (2009), Experimental Study of the QCD Phase Diagram & Search for the Critical Point, URL `https://drupal.star.bnl.gov/STAR/starnotes/public/sn0493`.

[18] L. Adamczyk et al. (STAR Collaboration), Phys. Rev. C **96**, 044904 (2017).

[19] B. I. Abelev et al. (STAR Collaboration), Phys. Rev. C **79**, 034909 (2009).

[20] M. Anderson et al., Nucl. Instrum. Methods A **499**, 659 (2003).

[21] STAR Note **SN0621** (2004), STAR TOF Proposal, URL `https://drupal.star.bnl.gov/STAR/starnotes/public/sn0621`.

[22] Z. Tang, Y. Xu, L. Ruan, G. van Buren, F. Wang, and Z. Xu, Phys. Rev. C **79**, 051901(R) (2009).

[23] L. Adamczyk et al. (STAR Collaboration), Phys. Lett. B **771**, 13 (2017).

[24] T. Sjöstrand, P. Edén, C. Friberg, L. Lönnblad, G. Miu, S. Mrenna, and E. Norrbin, Comput. Phys. Commun. **135**, 238 (2001).

[25] H. Agakishiev et al. (STAR Collaboration), Phys. Rev. D **83**, 052006 (2011).

[26] R. E. Nelson, R. Vogt, and A. D. Frawley, Phys. Rev. C **87**, 014908 (2013).

[27] G. A. Alves, S. Amato, J. C. Anjos, J. A. Appel, J. Astorga, S. B. Bracker, L. M. Cremaldi, W. D. Dagenhart, C. L. Darling, R. L. Dixon, et al. (Fermilab E769 Collaboration), Phys. Rev. Lett. **77**, 2388 (1996).
S. P. K. Tavernier, Rep. Prog. Phys. **50**, 1439 (1987).
L. Adamczyk et al. (STAR Collaboration), Phys. Rev. D **86**, 072013 (2012).
A. Adare et al. (PHENIX Collaboration), Phys. Rev. Lett. **97**, 252002 (2006).

[28] M. L. Miller, K. Reygers, S. J. Sanders, and P. Steinberg, Annu. Rev. Nucl. Part. Sci. **57**, 205 (2007).

[29] R. Rapp and H. van Hees, Phys. Lett. B **753**, 586 (2016).
R. Rapp, private communications (2017).

[30] S. Endres, H. van Hees, J. Weil, and M. Bleicher, Phys. Rev. C **91**, 054911 (2015).
S. Endres, H. van Hees, and M. Bleicher, Phys. Rev. C **94**, 024912 (2016).

[31] R. Rapp and J. Wambach, Eur. Phys. J. A **6**, 415 (1999).

[32] E. L. Bratkovskaya, private communication (2018).

[33] H. Specht (NA60 Collaboration), AIP Conf. Proc. **1322**, 1 (2010).

[34] P. M. Hohler and R. Rapp, Phys. Lett. B **731**, 103 (2014).